

Exceptional hyperbolic 3-manifolds

David Gabai* and Maria Trnkova**

Abstract. We correct and complete a conjecture of D. Gabai, R. Meyerhoff and N. Thurston on the classification and properties of thin tubed closed hyperbolic 3-manifolds. We additionally show that if N is a closed hyperbolic 3-manifold, then either $N = Vol3$ or N contains a closed geodesic that is the core of an embedded tube of radius $\log(3)/2$.

Mathematics Subject Classification (2010). 57M50; 57-04.

Keywords. Hyperbolic three-manifolds, Snap, length and ortholength spectra.

1. Introduction

An *exceptional* hyperbolic 3-manifold is a closed hyperbolic 3-manifold which does not have an embedded hyperbolic tube of radius $\log(3)/2$ about its shortest geodesics. These manifolds were introduced in [9] where geometric and topological rigidity theorems were proven for nonexceptional manifolds. All manifolds in this paper are orientable. A detailed investigation of exceptional manifolds was conducted in [12] where the corresponding rigidity theorems were extended to all closed hyperbolic 3-manifolds. Those results in turn were used in [10] to prove the Smale conjecture for closed hyperbolic 3-manifolds, i.e. the inclusion $\text{Isom}(N) \rightarrow \text{Diff}(N)$ is a homotopy equivalence. Properties of exceptional manifolds were also used in [12] (in conjunction with [13]) to establish a lower bound on the volume of a closed hyperbolic 3-manifold, giving a 100+ improvement on the previously known lower bound. They were used in the work of Agol [1] and Agol–Dunfield [3] to improve the lower bound and give other estimates that were essentially used in [11] to show that the Weeks manifold is the unique closed hyperbolic 3-manifold of minimal volume. Properties of exceptional manifolds were also used in [2] to give volume bounds for other classes of 3-manifolds.

An exceptional manifold N gives rise to a *marked* 2-generator subgroup G of $\pi_1(N)$ generated by elements f and w where the axis $\delta_0 \subset \mathbb{H}^3$ of f projects to a

*The first author was partially supported by grants NSF DMS-0854969 and NSF DMS-1006553.

**The second author was partially supported by the grant NSF DMS-0854969 and by grant P201/11/0356 of The Czech Science Foundation.

shortest geodesic of N and the element w sends δ_0 to a nearest covering translate δ_1 with $d(\delta_0, \delta_1) \leq \log(3)$. In [12] the set of marked 2-generator groups arising from exceptional manifolds is identified with a subset $S = \exp(T)$ of a compact region of \mathbb{C}^3 . Furthermore this region can be chopped up into about a billion regions and that any marked 2-generator group arising as above lies in one of seven small *exceptional regions* $X_i, i = 0, \dots, 6$. Each such region X has a *quasi-relator* $r(X)$, i.e. a word in $f, w, F = f^{-1}, W = w^{-1}$ that is very close to the identity at all points inside the region X . For more details see Chapters 0 and 1 of [12]. The authors of [12] made the following conjectures about the exceptional regions and exceptional manifolds:

Conjecture (Exceptional manifolds conjecture). *Each exceptional box $X_i, 0 \leq i \leq 6$, contains a unique element s_i of S . Further, if $\{G_i, f_i, g_i\}$ is the marked group associated to s_i then $N_i = \mathbb{H}^3/G_i$ is a closed hyperbolic 3-manifold with the following properties:*

- (i) N_i has fundamental group $\langle f, w; r_1(X_i), r_2(X_i) \rangle$, where $r_1(X_i), r_2(X_i)$ are the quasi-relators associated to the box X_i .
- (ii) N_i has a Heegaard genus-2 splitting realizing the above group presentation.
- (iii) N_i nontrivially covers no manifold.
- (iv) N_6 is isometric to N_5 .
- (v) If (L_i, D_i, R_i) is the parameter in T corresponding to s_i , then L_i, D_i, R_i are related as follows:

$$\begin{array}{ll} \text{For } X_0, X_5, X_6, & L = D, R = 0 \\ \text{For } X_1, X_2, X_3, X_4, & R = L/2. \end{array}$$

It was shown in [12] that for each j there is a Heegaard genus-2 manifold M_j with presentation as in (i). Also the closed hyperbolic 3-manifold Vol3 is the unique exceptional manifold N_0 corresponding to the region X_0 and (v) holds for X_0 .

K. Jones and A. Reid [16] proved that N_0 nontrivially covers no manifold and found arithmetic hyperbolic manifolds N_i for all the regions $X_i, i = 0, 1, 2, 4, 5, 6$. They also showed that the exceptional manifolds N_5 and N_6 are isometric.

The manifold N_3 is described by M. Lipyanskiy experimentally in [17].

A. Champanerkar, J. Lewis, M. Lipyanskiy and S. Meltzer [7] proved that each exceptional region contains a unique hyperbolic 3-manifold N_i . They also established properties (i) and (ii) for all the N_i 's and (v) for all the X_i 's. As each N_i is a rational homology 3-sphere, they observe that no N_i can cover a non orientable 3-manifold.

A. Reid [7] proved that the manifolds N_1 and $N_5 = N_6$ nontrivially cover no manifold.

What needs to be done. To complete the proof of the Exceptional manifolds conjecture, it suffices to show that the manifolds N_2 , N_3 and N_4 nontrivially cover no orientable manifold. The main result of this paper is a positive proof of this statement (i.e. conjecture (iii)) as modified by the following result.

Theorem 1.1. *If N_i is an exceptional manifold and $p : N_i \rightarrow M$ is a nontrivial covering projection, then up to conjugacy either $p : N_2 \rightarrow m010(-2, 3)$ or $p : N_4 \rightarrow m371(1, 3)$. Furthermore, any two such coverings (for a given domain and range) are topologically conjugate. Finally for each p , $\deg(p) = 2$.*

Remark 1.2. i) For a given $N_i, i = 2, 4$ there are three different homotopy classes of covering projections as above.

ii) The manifolds $m010(-2, 3)$ and $m371(1, 3)$ are given by SnapPea notation.

Remark 1.3. Neither of $m010(-2, 3)$, $m371(1, 3)$ are exceptional manifolds as their shortest geodesics have all tube radii $> \log(3)/2$.

Corollary 1.4. *Any exceptional manifold is isometric to one of N_0, N_1, N_2, N_3, N_4 , or N_5 .*

In the course of proving Theorem 1.1 we obtain the following.

Theorem 1.5. *If $N_i \neq N_0$, then some geodesic in N_i is the core of an embedded tube of radius $\log(3)/2$.*

Corollary 1.6. *$Vol3$ is the unique closed hyperbolic 3-manifold such that no closed geodesic is the core of an embedded tube of radius $\log(3)/2$.*

The proofs of Theorem 1.1 and 1.5 require rigorous computer assistance. They are motivated by output from the computer programs Snap [14] and SnapPea [21]. The program Snap studies arithmetic and numerical invariants of hyperbolic 3-manifolds and is based on the program SnapPea and on the number theory package Pari. SnapPea was written by Jeff Weeks for studying hyperbolic 3-manifolds and Pari calculates arithmetic and number theoretic functions with high precision.

In Section 2 we use the length and ortholength information provided by Snap for the manifolds $N_i, i = 2, 3, 4$ to conclude that N_3 nontrivially covers no manifold and that N_2, N_4 can only nontrivially cover a manifold via a special 2-fold one. Rigorously verifying output of SnapPea we then show that these manifolds actually have 2-fold quotients and they are exactly as in Theorem 1.1.

In order to make our results rigorous we have to check data from Snap. Snap makes all calculations with high precision and works well in practice but some algorithms (like algorithms for length and ortholength spectra) depend on the limitations of fixed-precision floating point computations. Rigorous evaluations of the length and ortholength spectra for the manifolds N_i are also needed to prove Theorem 1.5 and Remark 1.3. The second author wrote a package in *Mathematica* to

rigorously compute length and ortholength spectra for manifolds. This program can be used independently of this paper. The theoretical part of the algorithm, together with an explanation of its rigor, is given in Section 3.

Acknowledgements. M. Trnkova is very thankful to J. Weeks, N. Dunfield and C. Hodgson for their help with the computer program Snap, the Mathematics Department of Princeton University for their hospitality, the Institute for Advanced Study for the use of their computer cluster and Caltech for their hospitality during the final preparation of this manuscript. Maria is also very grateful to her advisor David Gabai for inspiration, guidance and support. She was a visiting student research collaborator of D. Gabai at Princeton University during the preparation of this manuscript and reported on these results at the NSF sponsored March 14–16, 2011 FRG conference in Princeton. The authors are thankful to a referee for the careful reading and very many constructive comments.

2. Ortholines of thick tube geodesics

This chapter completes the proof of Theorem 1.1 assuming the correctness of various results of Snap up to 50 decimal places. In the next chapter we rigorously check the needed data.

Recall the following three facts from [7]. For each exceptional region X_i , $i = 2, 3, 4$, there is a unique exceptional manifold N_i . Closed hyperbolic 3-manifolds $s778(-3, 1)$ and $v2018(2, 1)$ from SnapPea’s census are isometric to N_2 . There are no manifolds in SnapPea’s census isometric to N_3 or N_4 because of their large volumes.

Matrix representatives for the generators f, w of the fundamental group G_i depend only on the three complex parameters L', D', R' from the exceptional region X_i [12]:

$$f = \begin{pmatrix} \sqrt{L'} & 0 \\ 0 & 1/\sqrt{L'} \end{pmatrix} \quad (2.1)$$

$$w = \begin{pmatrix} \frac{\sqrt{R'}(\sqrt{D'}+1/\sqrt{D'})}{2} & \frac{\sqrt{R'}(\sqrt{D'}-1/\sqrt{D'})}{2} \\ \frac{(\sqrt{D'}-1/\sqrt{D'})}{2\sqrt{R'}} & \frac{(\sqrt{D'}+1/\sqrt{D'})}{2\sqrt{R'}} \end{pmatrix} \quad (2.2)$$

For example, the region X_2 is approximately bounded by:

$$\begin{array}{llll} l'_{min} = -1.78701 & l'_{max} = -1.78527 & t'_{min} = -2.27253 & t'_{max} = -2.27130 \\ d'_{min} = -1.07428 & d'_{max} = -1.07273 & b'_{min} = -2.71846 & b'_{max} = -2.71736 \\ r'_{min} = 0.74163 & r'_{max} = 0.74301 & a'_{min} = -1.52929 & a'_{max} = -1.52832. \end{array}$$

The quasi-relators $r_1(X_i), r_2(X_i)$ are relators of G_i at some triple $(L'_i, D'_i, R'_i) \in X_i$, $L' = l' + t'$, $D' = d' + b'$, $R' = r' + a'$. K. Jones and A. Reid [16] showed that a two generator group can be determined up to conjugacy by the triple of traces $(\text{tr } f^2, \text{tr } w^2, \text{tr } f^2 w^2)$. This triple generates a number field which is the invariant trace field.

[7] computed the trace triple $p = \text{tr } f$, $q = \text{tr } w$, $r = \text{tr } f^{-1} w$ up to high precision for all exceptional manifolds, e.g. 100 significant digits, and represented them as roots of polynomials over integers. Therefore we can get generators f, w with high precision as well. The initial triple and trace triple are connected by equations:

$$L' = \left(\frac{p \pm \sqrt{p^2 - 4}}{4} \right)^2$$

$$D' = \left(\frac{q\sqrt{R'} \pm \sqrt{q^2 R' - (1 + R')^2}}{1 + R'} \right)^2$$

$$R' = \frac{qL' - r\sqrt{L'}}{r\sqrt{L'} - q}$$

After calculating entries of the generators (2.1), (2.2) we can determine a manifold in Snap which is isometric to N_i . We refer to this manifold as N_i . For the manifold N_i Snap calculates length and ortholength spectra. Our proof of Theorem 1.1 is based on analyzing this information for the manifolds N_2, N_3, N_4 .

2.1. Manifold N2. For the region X_2 there exists a unique manifold N_2 isometric to $s778(-3, 1), v2018(2, 1)$ [7]. The fundamental group of this manifold is:

$$\langle f, w \mid FwfwfWffWfwfwFww, FFwFFwFwfwfwFww \rangle .$$

The triple (L', D', R') from the exceptional box $X_2 \subset C^3$ is presented by roots of polynomials over integers. Therefore we can get entries of generators with any desired precision. We display here only 5 decimal digits.

$$f = \begin{pmatrix} 0.74293 - 1.52908i & 0 + 0i \\ 0 + 0i & 0.25706 + 0.52908i \end{pmatrix}$$

$$w = \begin{pmatrix} 0.39135 - 0.96022i & -0.30677 - 1.26724i \\ 0.59162 - 0.48807i & 0.60864 - 0.03977i \end{pmatrix}$$

According to [16] and Snap the volume of N_2 is 3.6638... The orientable closed hyperbolic 3-manifold $m003(-3, 1)$ has the smallest volume 0.9427... [11]. So, the manifold N_2 is not a p -fold cover of an orientable closed hyperbolic manifold M if $p > 3$. Our analysis of possible 2-fold and 3-fold covers $p : N_2 \rightarrow M$ splits into two cases: first, when M is not an exceptional manifold, and second, when M is an exceptional manifold.

Case 1. If M is not an exceptional manifold, then any shortest closed geodesic of the underlying manifold M must have a tube of radius more than $\log 3/2$ [12]. Consequently, any component δ of its preimage in N_2 must be a closed geodesic with a tuberradius $> \log 3/2$. Since the density of the volume of a tube W about a geodesic in N_2 is less than or equal to the 0.9 by [19] it follows that $\text{volume}(W) < 3.3341$. Hence any geodesic in N_2 with tuberradius $> \log 3/2$ must have length < 3.18385 . Recall that for a tube W we have the equality $\text{volume}(W) = \pi l \sinh^2 r$, where l is the length of the core geodesic and r is the radius of the tube.

From Snap we get the list of all geodesics of length up to 3.18385 of manifold N_2 . Table 1 displays only the first eighteen geodesics from this list.

orbit	geodesic length	shortest ortholine	geodesic number
0	1.06128-2.23704*i	1.07253-1.94716*i	0,1,3,6,7,8
1	1.06128+2.23704*i	1.52857-1.14372*i	2,4,5
2	1.76275+3.14159*i	1.06128+2.23704*i	9,10,11
3	2.13862-0.79928*i	0.95994+1.31100*i	12,13,14,15,16,17
...			

Table 1. Length spectrum for N_2

Here we adapt Snap terminology. The *orbits* are given by the action of $\text{Isom}(N_2)$ on N_2 . An *ortholine* (also called *orthocurve* in the literature, e.g. [12]) is a geodesic segment which runs perpendicular from one closed geodesic to itself or from one geodesic to another. Its *length* (also called the *orthodistance* in [12]) is a complex number whose imaginary part is well defined mod 2π if either both geodesics are oriented or the curve goes from a geodesic to itself. Note that the *tube radius* of a geodesic (we call it also *injectivity radius* according to Snap terminology) is one half of the real length of a shortest ortholine to itself. Also the “shortest ortholine” in Table 1 (and Tables 5, 10) refers to a shortest ortholine from a geodesic to itself. Geodesics which do not appear in the Table 1 have shortest ortholines to itself of length less than $\log(3) = 1.0986\dots$, hence have tube radii $< \log(3)/2$. Therefore only geodesics in orbit [1] have tube radius $\geq \log(3)/2$ and these have tube radii approximately 0.764285. According to Snap, the real length of the shortest ortholine between any two distinct elements of orbit [1] is 0.88137. This implies that if $p : N_2 \rightarrow M$ is a non trivial covering projection, then it cannot happen that $p(\delta) = p(\delta')$, where δ, δ' are distinct elements of orbit [1] and $p(\delta)$ is a shortest geodesic of M .

Let δ denote an element of orbit [1]. After fixing a normal vector z to δ and an orientation on δ , then the initial and final points of an oriented ortholine respectively naturally determine complex numbers (also known as the *basings*) well defined up to $\text{length}(\delta)$. Indeed, if the initial (resp. final) point corresponds to the number v (resp. w), then translating z by a distance v (resp. w) along δ takes z to the initial

(resp. minus the final) tangent vector to the ortholine. The following Table 2 lists the ortholine spectrum to δ for ortholines whose real length is at most 2.

ortholine length	initial point of ortholine	final point of ortholine
$1.52857-1.14372*i$	$-0.06128-0.99023*i$	$0.46936+0.12829*i$
$1.52857-1.14372*i$	$-0.06128+2.15137*i$	$0.46936-3.01330*i$
$1.76275+3.14159*i$	$0.20404+1.13983*i$	$0.20404-2.00176*i$
$1.76275+3.14159*i$	$-0.32660+0.02131*i$	$-0.32660-3.12028*i$
$1.96864+2.53545*i$	$-0.06128+0.58057*i$	$0.46936+1.69909*i$
$1.96864+2.53545*i$	$-0.06128-2.56102*i$	$0.46936-1.44250*i$
...		

Table 2. Orthospectrum of a geodesic from orbit [1] for N_2

The information of Table 2 is schematically drawn in Figure 1. Observe that the union of the first and the third pairs of ortholines each forms a closed geodesic as the complex parts of their endpoints differ by π , while the other ortholines are closed geodesics themselves.

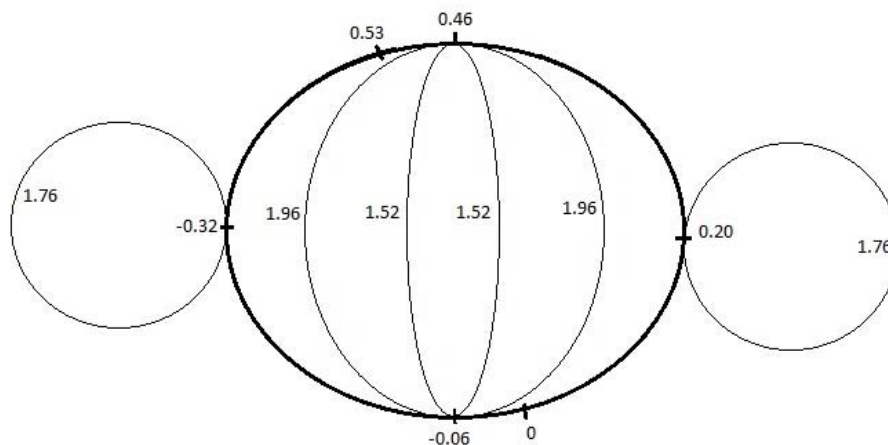


Figure 1. Ortholines of a geodesic from orbit [1] for N_2 .

We now show that N_2 does not 3-fold cover any manifold M . If so, then as discussed above some geodesic in orbit [1], say δ , 3-fold covers a shortest geodesic κ of M . Let ω be a shortest oriented ortholine from κ to itself. As ω is the image of an interval, its preimage will consist of three ortholines connecting δ to itself, whose initial points will be spaced at real distance $(\text{Re}(\text{length}(\delta)))/3$ along δ . Since each lift

will correspond to a shortest ortholine of δ to itself, this contradicts the ortholine spectrum given in Table 2.

Notice that the ortholine spectrum is not inconsistent with the existence of a 2-fold covering space. We searched the SnapPea census for manifolds M with $\text{volume}(M) = \text{volume}(N_2)/2$, then applied the covering space command to create 2-fold covers and then looked for manifolds whose first homology agreed with that of N_2 . We used SnapPy [8] to discover that $m010(-2, 3)$ has three double covers and one of them, denoted $'m010 \sim 0(1, 0)'$, has fundamental group isomorphic to that of $\pi_1(N_2)$. Next we applied SnapPy to show that the double cover $'m010 \sim 0(1, 0)'$ is isometric to manifolds $s778(-3, 1)$, $v2018(2, 1)$. This proves the existence of a degree-2 covering map $p : N_2 \rightarrow m010(-2, 3)$.

Now consider any 2-fold covering $q : N_2 \rightarrow M$. The fundamental group $\pi_1(N_2)$ is a subgroup of index 2 of $\pi_1(M)$ and hence is normal which implies that all 2-fold covers arise as free \mathbb{Z}_2 symmetries of N_2 . Orbit [1] has three geodesics. Therefore any free \mathbb{Z}_2 symmetry takes one of them onto itself in orientation preserving manner. Now looking at the orthospectrum of orbit [1] (see Table 3) we see that there is at most one non-trivial way to map a geodesic from orbit [1] onto itself such that orientation is preserved and its ortholines are mapped onto ortholines. At the same time the other two geodesics from orbit [1] are each mapped to the other. Thus there are no more than three free \mathbb{Z}_2 symmetries of N_2 .

From Snap we know the symmetry group of N_2 . Inspection of the isometry group shows that exactly three symmetries are free \mathbb{Z}_2 :

- (1) $f \rightarrow WfWWffW$, $w \rightarrow WfWFWF$,
- (2) $f \rightarrow fwfWfw$, $w \rightarrow fWfWffW$,
- (3) $f \rightarrow wFFwFWF$, $w \rightarrow wFFwwfw$.

Snap uses labels 2, 4, 5 for the geodesics of orbit [1]. The first isometry (resp. second, third) preserves the geodesic number 4 (resp. 5, 2). These geodesics have the following representations in terms of generators of the fundamental group:

$$2 \rightarrow WF, \quad 4 \rightarrow WfW, \quad 5 \rightarrow ffW.$$

Using these three isometries (1), (2), (3) we can map a geodesic of orbit [1] to any other geodesic of the same orbit. It follows that q is conjugate to p where the conjugating map is one of these isometries.

Case 2. We move to the case $p : N_2 \rightarrow M$ when M is an exceptional manifold.

The paper [12] proves that if M is an exceptional manifold, then there is another exceptional manifold N with a marked 2-generator group that covers M . Such an N arises from a parameter in one of the seven exceptional boxes. The fundamental group of N is generated by two elements f, w , where f is a hyperbolic element whose axis B projects to a shortest geodesic and w is a hyperbolic element which

takes B to a nearest translate. In particular N and M have shortest geodesics of the same length. We now show that $N = N_2$. By [11] we know that $vol(N) > 0.9427$. This would imply that the ratio $vol(N_2)/vol(N) = a/b$, where a, b are integers at most 8, which is not true as we know from [7] all the 7 possibilities for N . Since $N = N_2$ any element γ of orbit [0] maps with degree-1 to a shortest geodesic $\kappa \subset M$. Furthermore, any shortest ortholine for κ has the same real length 1.07253 of a shortest self ortholine for γ .

ortholine length	initial point of ortholine	final point of ortholine
0.88137-1.57080*i	2: 0.20404+1.13983*i	4: 0.32660-2.40328*i
0.88137-1.57080*i	2: 0.20404-2.00176*i	4: 0.32660+0.73831*i
0.88137-1.57080*i	4:-0.20404-0.38021*i	5:-0.32660-1.18408*i
0.88137-1.57080*i	4:-0.20404+2.76138*i	5:-0.32660+1.95751*i
0.88137+1.57080*i	2:-0.32660+0.02131*i	5: 0.20404+3.07603*i
0.88137+1.57080*i	2:-0.32660-3.12028*i	5: 0.20404-0.06557*i
...		

Table 3. Ortholine spectrum for orbit [1] of N_2 with ortholines of real length up to 1.4. For each ortholine integers 2, 4 or 5 on the left in second and third columns denote names of geodesics from orbit [1] where the ortholine has its endpoints.

It was shown before that $deg(p) \leq 3$. Thus the preimage of κ consists of γ together with other geodesics which together map with degree at most 3 to κ . There are no geodesics in N_2 with real length twice that of γ (see Table 1), thus the preimage of κ lies entirely in orbit [0]. The real length of shortest ortholines between sets of geodesics $\{0, 1, 3\}$ and $\{6, 7, 8\}$ is 0.21561 (see Table 4). It is less then the shortest ortholine ω of κ , therefore there is no 3-fold cover.

ortholine length	name of geodesic that contains initial point of ortholine	name of geodesic that contains final point of ortholine
0.21561-1.16921*i	0	1
0.21561-1.16921*i	1	3
0.21561+1.97238*i	0	3
0.21561+1.97238*i	6	7
0.21561+1.97238*i	6	8
0.21561+1.97238*i	7	8
...		

Table 4. Ortholine spectrum up to 1.07 for orbit [0] of N_2

these lengths is not a rational number a/b such that $a + b = n, n = 2, 3, 4, 5, 6, 7$. Therefore the preimage of κ must be either in orbit [1] or [3].

It cannot happen that δ_i is a degree-1 cover of κ because κ is a shortest geodesic in M but an image of a geodesic from orbit [0] is shorter than δ_i .

2.2.1. $\delta \in \text{Orbit [1]}$. Let δ denote an element of orbit [1]. Assume that $p : N_3 \rightarrow M$ and $p|\delta$ is a degree- x cover of κ where κ is a shortest geodesic in M and $x > 1$. Snap asserts that there is a unique ortholine σ of real length 1.81586... that starts and ends on δ (see Table 6). Table 7 shows that there is no ortholine of that real length between any distinct geodesics δ to δ' from orbit [1]. This contradicts the fact that the preimage of a shortest ortholine of κ has x ortholines between δ and δ' .

ortholine length	multiplicity
1.67039-2.41832*i	2
1.81586+0.21843*i	1
...	

Table 6. Orthospectrum up to 1.85 of a geodesic from orbit [1] for N_3

ortholine length between δ_1 and δ_2 from [1]	multiplicity
1.15910-0.00000*i	2
1.15910+3.14159*i	2
2.17052-0.51494*i	2
2.17052+0.51494*i	2
2.17052-2.62666*i	2
2.17052+2.62666*i	2
...	

Table 7. Orthospectrum up to 2.2 of two distinct geodesics from orbit [1] for N_3

2.2.2. $\delta \in \text{Orbit [3]}$. Now assume that δ is an element of orbit [3]. By Snap any two distinct geodesics from orbit [3] have an ortholine connecting them of real length less than $\log(3)$. This implies that only a single geodesic from orbit [3] can be a preimage of κ , hence we can assume that that geodesic is δ . Observe that $x > 2$ since δ is more than two times longer than a shortest geodesic of N_3 . On the other hand, by Snap, δ has only two shortest ortholines that begin and end on δ (see Table 8). This implies that $x \leq 2$ is a contradiction.

This means there is no chance that any closed geodesic or geodesics from orbits [1] or [3] can map onto a shortest geodesic κ of M and N_3 does not non-trivially cover any non-exceptional manifold.

ortholine length	multiplicity
$1.29867 \pm 2.03065 * i$	2
$1.29909 \pm 1.04518 * i$	2
...	

Table 8. Orthospectrum up to 1.3 of a geodesic from orbit [3] for N_3

We now consider the case that M is an exceptional manifold. As in the previous section we can assume that no other exceptional manifold can cover M . Thus a geodesic γ from orbit [0] of N_3 maps onto a shortest geodesic κ of M . Hence the real length of κ is not less than 1.21275. The preimage of a shortest ortholine ω of κ is a shortest ortholine of γ , $Relength(\omega) \geq 1.09488$. Then the maximum volume of a tube W around κ is not less than 1.26053. By [19] the volume of the tube W has density at most 0.91 in M and hence $vol(M) \geq 1.3851$. Therefore the $deg(p) \leq 5$.

There are no geodesics in N_3 with real length 2, 3, 4 or 5 times bigger than the real length of a single geodesic from orbit [0]. A preimage of κ lies entirely in orbit [0]. Table 9 shows that the real length of shortest ortholines between sets of geodesics $\{0, 1, 2\}$ and $\{3, 4, 5\}$ is 0.12450. It is less then the real length of the shortest ortholine ω , therefore there is no 3, 4 or 5-fold cover. There might be a 2-fold cover: one component of $p^{-1}(\kappa)$ is one of the geodesics 0, 1 or 2 and the other component is one of 3, 4 or 5. But since the complex lengths of geodesics 0, 1, 2 and 3, 4, 5 are conjugate (in Table 5 they marked by asterisk), it follows that every isometry that takes 0 to 3 (or 4, or 5) is orientation-reversing. Which would imply that the quotient is non-orientable and this is not allowed [7].

ortholine length	geodesic with initial point of ortholine	geodesic with final point of ortholine
$0.12450 - 1.05142 * i$	0	1
$0.12450 - 1.05142 * i$	1	2
$0.12450 + 1.05142 * i$	3	4
$0.12450 + 1.05142 * i$	4	5
$0.12450 - 2.09017 * i$	3	5
$0.12450 + 2.09017 * i$	0	2
...		

Table 9. Orthospectrum up to 1.09 for orbit [0] for N_3

There is no possibility that δ_i is a one-to-one cover of κ because κ is a shortest geodesic but the image of geodesics from orbit [0] is shorter than κ .

2.3.1. Orbit [1]. Shortest ortholines between different geodesics from orbit [1] have real length $0.95330 < \log(3)$. That is the reason why we can consider as a preimage of κ only a single geodesic δ from orbit [1]. Each geodesic δ_i from orbit [1] has only two shortest ortholines running to itself of length 1.90660 (see Table 11). These ortholines cannot be a preimage of any ortholine of κ under the projection p except if p is a double cover and δ_i is a double cover of κ .

ortholine length	multiplicity
1.90660+2.73377*i	2
2.04203+0.92305*i	4
...	

Table 11. Orthospectrum up to 2.2 for a geodesic from orbit [1] for N_4

We check all closed orientable hyperbolic manifolds from SnapPea’s census which can be potentially a double quotient of N_4 using volume and the first homology group $H_1 = \mathbb{Z}_4 \oplus \mathbb{Z}_{12}$. We get only one such manifold $m371(1, 3)$. One of its double covers ‘ $m371 \sim 2(1, 0)$ ’ has fundamental group

$$\langle a, b \mid aabbaBabaBabbaabAbabABAbABAbabAb, \\ aabbaabAbabABAbABBAABBAAbABAbabAb \rangle$$

which is isomorphic to $\pi_1(N_4)$:

$$a \rightarrow w, \quad b \rightarrow F, \quad \text{and} \quad w \rightarrow a, \quad f \rightarrow B.$$

This proves the existence of a double quotient of N_4 .

2.3.2. Orbit [3]. The distance between distinct geodesics from orbit [3] is $0.68306 < \log(3)$ and a preimage of κ can be only a single geodesic δ from orbit [3]. Each geodesic δ_i from [3] has only two shortest ortholines of length 1.36612 (see Table 12). Therefore these ortholines cannot be preimages of any ortholine of κ unless there is a 2-fold cover. In the case of a 2-fold cover we analyse Table 13. One geodesic from orbit [3] could cover κ while the other two geodesics from [3] will project onto one geodesic and will have a shortest ortholine of real length 0.68306. This ortholine would be a simple closed geodesic that is shorter than κ . We get a contradiction to the assertion that κ is the shortest geodesic.

2.3.3. Orbit [4]. Distances between distinct geodesics from orbit [4] are 0.15119, 0.57139 or 0.68605, all less than $\log(3)$. A preimage of κ can be only a single

geodesic δ from orbit [4]. The only possible quotients of δ that must be considered are 3, 4, 5, 6 and 7. There is no 2-fold cover since δ is more than two times longer than a shortest geodesic of N_4 . Each geodesic δ_i from orbit [4] has only two shortest ortholines of length 1.16156 (see Table 14). Therefore these ortholines cannot be preimages of any underlying ortholine of κ .

ortholine length	multiplicity
1.36612-2.17271*i	2
1.93611+2.16313*i	4
...	

Table 12. Ortholine spectrum up to 2.1 for a geodesic from orbit [3] for N_4

ortholine length	initial point of ortholine	final point of ortholine
0.68306-1.08635*i	12: 0.43080+1.52064*i	14:-0.37287-2.03502*i
0.68306-1.08635*i	12: 0.43080-1.62096*i	14:-0.37287+1.10657*i
0.68306-1.08635*i	13:-0.03978-1.42844*i	14: 0.58043+2.47346*i
0.68306-1.08635*i	13:-0.03978+1.71315*i	14: 0.58043-0.66813*i
0.68306+2.05524*i	12: 1.38410+2.88752*i	13: 0.91352+3.08004*i
0.68306+2.05524*i	12: 1.38410-0.25407*i	13: 0.91352-0.06156*i
1.36612-2.17271*i	12: 0.43080+1.52064*i	12: 0.43080-1.62096*i
1.36612-2.17271*i	12: 1.38410+2.88752*i	12: 1.38410-0.25407*i
1.36612-2.17271*i	13:-0.03978-1.42844*i	13:-0.03978+1.71315*i
1.36612-2.17271*i	13: 0.91352-0.06156*i	13: 0.91352+3.08004*i
1.36612-2.17271*i	14:-0.37287-2.03502*i	14:-0.37287+1.10657*i
1.36612-2.17271*i	14: 0.58043-0.66813*i	14: 0.58043+2.47346*i
...		

Table 13. Orthospectrum up to 1.5 for orbit [3] for N_4 For each ortholine, integers 12, 13 or 14 on the left in the second and third columns denote names of geodesics from orbit [3] where the ortholine has its endpoints.

2.3.4. Orbit [18]. The distances between different geodesics from orbit [18] is $0.70700 < \log(3)$ and a preimage of κ can be only a single geodesic δ from orbit [18]. Possible quotients of δ_i are 4, 5, 6 and 7. There are not 2 and 3-fold covers since δ is more than three times longer than a shortest geodesic of N_4 . Each geodesic δ from [18] has only three ortholines of length 1.23288 (see Table 15). Hence these ortholines cannot be preimages of any underlying ortholine of κ except if p is a 3-fold cover. But the 3-fold case is excluded.

It means there is no chance that a closed geodesic or geodesics from orbits [1], [3], [4] or [18] can map onto a shortest geodesic κ of M except if M is the manifold $m371(1, 3)$.

ortholine length	multiplicity
1.16156-1.35749*i	2
1.44803+1.88714*i	2
...	

Table 14. Orthospectrum up to 1.7 for a geodesic from orbit [4] for N_4

ortholine length	multiplicity
1.16280+1.53153*i	6
1.23288-1.97709*i	3
...	

Table 15. Orthospectrum up to 1.78 for a geodesic from orbit [18] for N_4

In a similar way as we did for N_2 we can show that N_4 does not have any other 2-fold quotients. As for N_2 we see from the orthospectrum of orbit [1] in Table 16 that there are at most three free \mathbb{Z}_2 symmetries of N_4 . Geodesics of orbit [1] have the following representations in terms of generators of the fundamental group:

$$6 \rightarrow FwWf, \quad 7 \rightarrow WfWf, \quad 8 \rightarrow WfWF.$$

From Snap we got three symmetries that map an element of the orbit [1] to any other element of the same orbit:

- (1) $f \rightarrow WffWWfWfW, \quad w \rightarrow WffWfWfWF,$
- (2) $f \rightarrow wFWFwFWfWF, \quad w \rightarrow wFWFwFWFw,$
- (3) $f \rightarrow fwFwfwFFw, \quad w \rightarrow fwFwfwfwfW.$

We rigorously checked this by hand by finding automorphisms of $\pi_1(N_4)$ that have this property. It follows that a projection q is conjugate to p with the conjugating map being one of these three isometries.

Finally we consider the case when M is an exceptional manifold. A geodesic γ from orbit [0] of N_4 maps onto a shortest geodesic κ of M and real length $\kappa \geq 1.20475$. The preimage of a shortest ortholine ω of κ is a shortest ortholine of γ . Thus $\text{Relength}(\omega) \geq 1.09508$. The maximum volume of tube W around κ is more than or equal to 1.25272. By [19] the volume of the tube W has density at most 0.91 in M and hence $\text{vol}(M) \geq 1.37661$. Therefore the $\text{deg}(p) \leq 5$.

There are no geodesics of length 2, 4 or 5 times of γ . There are two orbits [14], [15] of geodesics with real length three times bigger than length of a single

geodesic γ from orbit [0]. Their shortest ortholines are of length 0.90630 and 1.07165. Both are less than $\text{Relength } \omega$. Therefore a preimage of κ lies entirely in orbit [0].

The real length of shortest ortholines between the sets of geodesics $\{0, 1, 3\}$ and $\{6, 7, 8\}$ is 0.13192 (see Table 17). It is less than the shortest ortholine ω of κ , therefore there is no n -fold cover when $n \geq 3$. There might be a 2-fold cover $p : N_4 \rightarrow M$ which appears from a free \mathbb{Z}_2 action on M . We consider the possible quotients of orbit [1] which has three geodesics of real length 1.36612. At least one of them will cover a geodesic of real length 0.68306 and that is less than the length of a shortest geodesic 1.20475. Therefore, N_4 nontrivially covers no exceptional manifold if the length and ortholength spectra are rigorous.

ortholine length	initial point of ortholine	final point of ortholine
0.95330+1.36689*i	6: 0.86526-2.08100*i	7: 0.47302+1.69236*i
0.95330+1.36689*i	6: 0.86526+1.06059*i	7: 0.47302-1.44923*i
0.95330+1.36689*i	7:-0.21004-0.36288*i	8: 0.65655-1.18161*i
0.95330+1.36689*i	7:-0.21004+2.77871*i	8: 0.65655+1.95999*i
0.95330-1.77471*i	6: 0.18220-0.99465*i	8:-0.02651+3.04634*i
0.95330-1.77471*i	6: 0.18220+2.14695*i	8:-0.02651-0.09525*i
...		

Table 16. Orthospectrum up to 1.8 of orbit [1] for N_4

ortholine length	initial point of ortholine	final point of ortholine
0.13192+1.05846*i	0: 0.53079-1.42015*i	1: 0.24072+1.64443*i
0.13192+1.05846*i	1:-0.36165-2.23240*i	2:-0.56763+0.84640*i
0.13192+1.05846*i	3: 0.20134+1.55778*i	4: 0.52205-2.98266*i
0.13192+1.05846*i	4:-0.08032-0.57631*i	5: 0.66320+2.76679*i
0.13192-2.08313*i	0:-0.07159+0.98620*i	2: 0.03475-1.55995*i
0.13192-2.08313*i	3: 0.80372-0.84857*i	5: 0.06082-1.11004*i
...		

Table 17. Orthospectrum up to 1.09 of orbit [0] for N_4

3. Rigorous length and ortholength spectra

In the previous section we used results obtained by Snap: Dirichlet domain, length and ortholength spectra, injectivity radii (also known as tube radii) to prove the theorem. That part was based on experimental data which are not rigorous (round-off

error was not considered). We took exactly the same input from Snap (face pairings) and found the list of geodesics and ortholines with exact round-off errors (we did all algebraic calculations with errors). Our results are identical to the ones obtained by Snap; that proves the theorem.

To check the results from Snap we wrote a package in *Mathematica* that calculates the length and ortholength spectra for the given geodesic. In this section we describe the theoretical part of our algorithm. Two files are attached to the arxiv version of this paper - *length.nb* (which contains the interface where you actually run the code together with the description of all necessary commands and options), *source_length.nb* includes a source code which is loaded by the first file in the beginning. Our package was written in order to find the geodesics and ortholines for manifolds N_2, N_3, N_4 but can be used for any other manifolds as well.

As for precision, *Mathematica* uses advanced algorithms to reach arbitrary precision during numerical evaluations. Therefore, the precision of our result is limited just by the precision of the input data (generators of a fundamental group, face pairings of a Dirichlet domain) and the computer memory. Also, the precision of the evaluation is being continuously updated when running the code. Our algorithm was tested on the cases of manifolds N_2, N_3, N_4 (and also other examples) and the results for geodesics and ortholines precisely agree with the data obtained by Snap version 1.11.3. For each manifold we calculate geodesic length, injectivity radius, etc. These numbers are never precise because the initial data have some errors. But because we keep track of the errors at all stages we know the round-off error also for these numbers. Therefore, it is trivial to check if the given number is smaller or bigger than some cutoff value (called precision in the code) within its precision (round-off error). Therefore, we can claim that our result is rigorous.

To get a sense of the number of computations involved, consider the manifold N_3 ; we want to calculate geodesics up to length 6.7243 and their tube radii. The Dirichlet domain that we use for N_3 has 36 faces. A lot of computations must be done to get the list of geodesics in this case. On the order of 10^8 group elements must be checked before we get a list of geodesics. It takes several hours for our package to get the list while Snap calculates this list in a few minutes, but reliability is our first priority. For the same manifold our package gives a list of geodesics with cut-off less than 4.0 in seconds.

We now discuss our algorithm for the manifolds $N_i, i = \{2, 3, 4\}$, where N_i is the unique exceptional manifold associated to the region X_i . Using the fundamental group of N_i , Snap finds a hyperbolic 3-manifold M_i . Of course, there is an isomorphism between fundamental groups of manifolds N_i and M_i . From Mostow's Rigidity Theorem [M, Th] it follows that these manifolds are homeomorphic.

For example, the fundamental group of M_2 is

$$\langle a, b \mid AbabaBaaBababAbb, AAbAAbbAbababAbb \rangle$$

and an isomorphism is $a \rightarrow f, b \rightarrow w$.

Let M be a hyperbolic three-dimensional manifold of finite volume. We use information about a Dirichlet domain of M from Snap to calculate the spectra and injectivity radii precisely. We use:

- fundamental group represented by generators a_i as matrices in $SL(2, C)$ with high precision,
- a matrix $c \in O(3, 1)$ conjugating between coordinates in which the base point of the Dirichlet domain is at the origin and the coordinates in which the generators for the fundamental group were originally given to the Dirichlet domain finding code,
- words for the face pairings.

An algorithm for the length spectrum is described in [15]. The difference of our algorithm from the one used in Snap is that we construct the Dirichlet domain for M in the projective ball model (also known as Beltrami's model or Klein's model). In this model we operate with matrices in $SL(2, C)$ which give smaller error than $O(3, 1)$ and it is easier to calculate hyperbolic distance, edges and planes there.

The algorithm requires a spine radius of our Dirichlet domain. The *spine radius* is defined as the infimum of the radii of all spines to the domain. We cannot get a spine radius of the Dirichlet domain from Snap. Therefore, we start with a construction of the Dirichlet domain for M and calculate a lower bound of its spine radius.

We recall the definition of the Dirichlet domain [6]. Let Γ be a group of isometries of the metric space (X, d) whose action is discontinuous. The *Dirichlet domain* of Γ centered at the point $x \in X$ is the subset

$$D_\Gamma(x) = \{y \in X : d(x, y) \leq d(g(x), y) \text{ for every } g \in \Gamma\},$$

consisting of those points $y \in X$ which are at least as close to x as to any other point of its orbit $\Gamma(x)$. In our notation we refer to $D_\Gamma(x)$ as D and always x will be a basepoint. In the case of hyperbolic space H^3 the set of points z that are at the same hyperbolic distance from x and y is a hyperbolic plane P_g and the set of z with $d_{\text{hyp}}(x, z) \leq d_{\text{hyp}}(y, z)$ is a hyperbolic half-space H_g delimited by this perpendicular bisector plane P_g . The Dirichlet domain D is a finite-sided polyhedron. The polyhedra gD with $g \in \Gamma$ form a tessellation of H^3 and gD is distinct from D unless $gx = x$.

For our purposes it is better to define the Dirichlet domain using half-spaces. The Dirichlet domain D of M with base point x is the intersection of the half-spaces H_g , for all covering transformations $g \in \Gamma$:

$$D = \bigcap_{g \in \Gamma} H_g.$$

Each hyperbolic isometry g has an axis A_g , that is a fixed geodesic under the isometry. In other words, to each transformation g there corresponds a geodesic A_g .

If we look for geodesics of length up to λ we have to consider all isometries g that move the basepoint x a distance less than s . This distance s depends on the cut-off length λ and the size of the Dirichlet domain, which is characterized by the spine radius.

3.1. Spine Radius. After giving some definitions we define a spine radius and introduce an algorithm for calculating it.

Each Dirichlet domain, with faces identified, specifies a cell decomposition K for M . A *spine dual to the Dirichlet domain* is a two-skeleton of a cell decomposition K' of M dual to K . All closed geodesics of M intersect a spine dual to the Dirichlet domain. The maximum distance from a point in the spine dual to the Dirichlet domain to the basepoint x is called the *radius*.

The *spine radius r of the Dirichlet domain* is the infimum of the radii of all spines dual to the domain.

The spine radius has a property that it equals to the *maximin edge distance* of the Dirichlet domain [15]. We use this fact to calculate a spine radius rather than its direct definition. The *maximin edge distance* is the maximum over all edges of the Dirichlet domain of the minimum distance between the basepoint x and an edge of D . Note that the spine radius is finite for all Dirichlet domains.

We explain the algorithm for the construction of the Dirichlet domain for a manifold M and use data about the Dirichlet domain obtained by Snap.

- First, we transform the $SO(3, 1)$ matrix c into $SL(2, C)$ and conjugate matrices a_i by the matrix c but continue to refer to them as a_i . After conjugating, the Dirichlet domain is centered at the point $O(0, 0, 1)$ in the upper-half space model U^3 .
- Represent all face pairing relations as matrices $g_j \in SL(2, C)$ (e.g., $j = \overline{1, 24}$ for the manifold M_2).
- Find the images $g_j(O)$ of the basepoint $O(0, 0, 1)$ under all face-pairings g_j in U^3 . They correspond to the basepoints of all neighbor domains. We calculate $g_j(O)$ via multiplication of quaternions:

$$g(w) = (\alpha \star w + \beta) \star (\gamma \star w + \delta)^{-1},$$

where $g = \begin{pmatrix} \alpha & \beta \\ \gamma & \delta \end{pmatrix} \in SL(2, C)$, $w = x + yi + zj$ and \star represents a multiplication of quaternions.

- In the paper [17] it is described how to get the set of all vertices of the Dirichlet domain. We follow this algorithm. Map O and $g_j(O)$ from the upper-half space U^3 into the projective ball model D^3 . There is an isometry $\varphi : D^3 \rightarrow U^3$ with inverse $\varphi^{-1} : U^3 \rightarrow D^3$:

$$\varphi(x + yi + zj) = \frac{(2x_0, 2y_0, x_0^2 + y_0^2 + z_0^2 - 1)}{1 + x_0^2 + y_0^2 + z_0^2}.$$

- All planes P_g which contain faces of the Dirichlet domain are bisecting planes between points $(0, 0, 0)$ and $\varphi^{-1}g_j(O)$.

$$P_g = \{r \in D^3 : \mathbf{n} \cdot r = t\}$$

where $\mathbf{n} = \varphi^{-1}g_j(O)$, $t = 1 - \sqrt{1 - |\varphi^{-1}g_j(O)|^2}$.

- A vertex $R = (r_1, r_2, r_3)$ defined by the intersection of three planes as a simultaneous solution of $\mathbf{n}_1 \cdot r = t_1$, $\mathbf{n}_2 \cdot r = t_2$ and $\mathbf{n}_3 \cdot r = t_3$. We discard a vertex which lie "above" some plane P_g .
- Each edge is defined by a couple of vertices. We check all pairs of vertices which share a common plane to see if they define an edge of the Dirichlet domain. We discard a line determined by two vertices if it lies in a single plane.
- For each edge we calculate a distance d from the basepoint (the origin) to the edge. First we find the endpoint of the perpendicular from the origin to the line containing the edge. If it lays between two vertices of the edge then d is the distance from the origin to the line containing the edge. Otherwise d is the distance to the closest vertex. Finally, we define the spine radius r as the maximum of these distances over all edges.

3.2. Geodesics. Now we are ready to sketch out the algorithm for computing a length spectrum of geodesics described in [15]. The general idea of our algorithm is the same but some steps were made differently. We overview the algorithm here with some additions.

Proposition. *To find all closed geodesics of length at most λ , it suffices to find all translates gD such that $d(x, gx) \leq 2 \cosh^{-1}(\cosh r \cosh(\lambda/2))$.*

Here r is the spine radius for the Dirichlet domain D centered at the point x . The metric d on the upper-half space is given by

$$\cosh d(x, y) = 1 + \frac{|x - y|^2}{2x_3y_3}.$$

We tile a region in H^3 around the Dirichlet domain D centered at the origin by all translates gD . These translations move the basepoint to a distance less than the distance defined in the above proposition. We are not interested in group elements g with $Relength(g) = 0$ or $Relength(g) > \lambda$ or whose axis does not pass within a distance r of the basepoint (every geodesic must intersect a spine radius r). The $Relength$ of a transformation g is the real part of the complex number

$$length(g) = 2 \operatorname{Arccosh} \frac{tr(g)}{2}.$$

The distance r from the basepoint to the axis of the isometry g is

$$r = \operatorname{Arccosh} \sqrt{\frac{\cosh d - \cos t}{\cosh s - \cos t}},$$

here $d = g(0, 0)$, $s + it = \operatorname{length}(g)$.

We want to find all geodesics that satisfy three constraints described above. The main idea of our algorithm is the following

- All the geodesics up to the cut-off λ correspond to group elements which can be constructed from the products of the face pairing relations of the domain. This multiplication forms a natural tree-like structure.
- We move in this tree and for any point check if it passes the base point distance constraint. If the answer is positive, we continue deeper in the tree from this point. Otherwise, we go back.
- If the geodesic moves the base point to a distance less than $d(x, gx)$ and in addition two other constraints are satisfied, we check if it is already in the list. If not, we add it.
- This algorithm is guaranteed to finish in finite time because there is just a finite number of group elements of the tree (which correspond to geodesics up to length λ) that move the basepoint to a distance smaller than cutoff.

There is no element that moves the basepoint of the Dirichlet domain a distance less than s , all of whose neighbors move the basepoint to a distance greater than s [15]. Hence our algorithm cannot miss any translation.

This tiling produces a so called *big list* of group elements g_i corresponding to all geodesics of length at most λ . This list might contain different group elements which correspond to the same geodesic. We want to have precisely one group element in each conjugacy class. Remove group elements that are just powers of others. Discard all conjugates, the inverse and its conjugates for each geodesic. The conjugacy is realized by an element h from the big list such that

$$d(x, gx) \leq 2 \cosh^{-1}(\cosh r \cosh(\lambda/4)).$$

We call *small list* the part of the big list which is left after eliminations of all duplicates. The small list has a length spectrum with correct multiplicities.

3.3. Ortholines. We want to find ortholines between closed geodesics A_f and A_g up to length δ and positions of their endpoints with angles on the geodesics. We look for them among ortholines between preimages of A_f , A_g and conjugates to A_g in the universal cover U^3 .

- (1) For easier calculations we map geodesic A_f (- axis of transformation f) onto geodesic $B_{0,\infty}$ by the inverse of transformation q :

$$q^{-1} : A_f \longrightarrow B_{0,\infty}, \quad q \in \text{Isom}(H^3),$$

$B_{0,\infty}$ is an oriented geodesic $\{(0, 0, z) : 0 < z < \infty\}$ and $(0, 0, 0)$ is its negative endpoint. The axis of transformation $f' = q^{-1} f q$ is $B_{0,\infty}$. We choose one of transformations q :

$$q = \begin{pmatrix} z_1 & z_0/(z_1 - z_0) \\ 1 & 1/(z_1 - z_0) \end{pmatrix},$$

where $z_i = \frac{f_1 - f_4 \pm \sqrt{(f_1 + f_4)^2 - 4}}{2f_3}$ are endpoints of A_f (i.e. fixed points of f which lie on the boundary of H^3). This transformation maps geodesic A_g onto the axis of transformation $g_0 = q^{-1} g q$, where $g_0 = \begin{pmatrix} g_{01} & g_{02} \\ g_{03} & g_{04} \end{pmatrix}$.

Special cases: If $f_3 = 0$ and $f_1 \neq 1$ then

$$q = \begin{pmatrix} 1 & \frac{f_1 f_2}{1 - (f_1)^2} \\ 0 & 1 \end{pmatrix}.$$

If $f_1 + f_4 = \pm 2$ then f is either a parabolic or a pure reflection and does not have an axis. In this case the algorithm will stop.

- (2) We choose a transformation $h \in \text{Isom}(H^3)$ such that $h : B_{0,\infty} \longrightarrow A_{g_0}$.

$$h = \begin{pmatrix} z_1 & z_0/(z_1 - z_0) \\ 1 & 1/(z_1 - z_0) \end{pmatrix},$$

where z_i are endpoints of A_{g_0} .

Again we have special cases: If $g_{03} = 0$ and $g_{01} \neq 1$ then

$$h = \begin{pmatrix} 1 & \frac{g_{01} g_{02}}{1 - (g_{01})^2} \\ 0 & 1 \end{pmatrix}.$$

If $g_{01} + g_{04} = \pm 2$ then g_0 is either a parabolic or a pure reflection and does not have an axis. In this case the algorithm will stop too.

- (3) We can calculate the distance between geodesics A_f and A_g . It is equal to the complex distance of an orthocurve from geodesic $B_{0,\infty}$ to A_{g_0} because isometries preserve distance. An ortholine between $B_{0,\infty}$ and A_{g_0} is an axis of transformation $k_0 = h\tau h^{-1}\tau$ and its length is twice bigger than the

distance d_0 (τ is a rotation around geodesic $B_{0,\infty}$). Hence, the distance d_0 is defined from the formula [4, 12, 15]:

$$\cosh d_0 = \cosh \text{distance}(B, h(B)) = \text{otr}(h),$$

where $\text{otr}(h) = h_1 h_4 + h_2 h_3$,

$$\tau = \begin{pmatrix} i & 0 \\ 0 & -i \end{pmatrix}.$$

- (4) In a similar way we calculate distances between A_f and axes of conjugacy of g . We conjugate element g_0 by group elements $p_i \in \text{Isom}(H^3)$ from the second “big list” and apply transformation q^{-1} . These transformations have the same axes as transformations $g_i = (q^{-1} p_i q) g_0 (q^{-1} p_i q)^{-1}$ which are also the images of the axis $B_{0,\infty}$ under transformations ph_i , where $ph_i = q^{-1} p_i q h$. Hence, distances d_i between A_f and axes of conjugacy of g defined from the formula:

$$\cosh d_i = \cosh \text{distance}(B, ph_i(B)) = \text{otr}(ph_i), \quad (i \geq 1).$$

Ortholines for these geodesics are axes of transformations $k_i = ph_i \tau (ph_i)^{-1} \tau$. The following lemma about conjugated group elements says how to get the second “big list”.

Proposition. *If g_1 and g_2 are two conjugate group elements such that the axis A_{g_1} corresponds to a geodesic within a distance r from the basepoint and axis A_{g_2} is within a distance δ from a fixed geodesic A_f , then there is a group element h such that $g_2 = h g_1 h^{-1}$ and*

$$d(x, hx) \leq \frac{1}{2}(\lambda_f + \lambda_g) + \delta + r.$$

Proof. We need only consider the situation when the axis A_f coincides with geodesic $B_{0,\infty}$. We are looking for ortholines that are at distance less than or equal to $\lambda_f/2$ from the basepoint x . Let Q be the end of the perpendicular from the basepoint x to axis A_{g_1} . There are infinitely many covering transformations that take A_{g_1} to A_{g_2} . We take one h that minimizes the distance between hQ and ortholine’s endpoint N . The length of geodesics A_{g_1} and A_{g_2} is λ_g , therefore the distance between N and hQ is less than or equal to $\lambda_g/2$. Then $d(Q, hQ) \leq d(x, M) + d(M, N) + d(N, hQ) + d(hQ, hx)$,

$$d(Q, hQ) \leq \lambda_f/2 + \delta + \lambda_g/2 + r. \quad \square$$

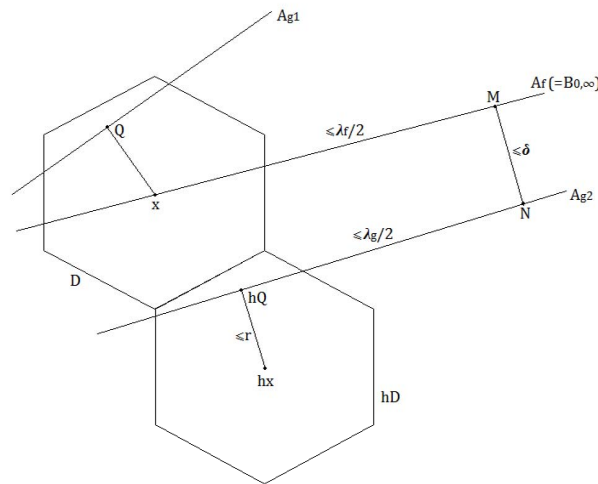


Figure 2. The distance from x to hx is less than or equal to $\frac{1}{2}(\lambda_f + \lambda_g) + \delta + r$, where λ_γ is the translation length of γ .

- (5) The position of an ortholine's endpoint on the geodesic A_f is a complex distance along geodesic $B_{0,\infty}$ from $B_{-1,1}$ to the ortholine between $B_{0,\infty}$ and A_{g_j} , ($j \geq 0$). In order to get this distance we fix orientation, choose a point and a based vector on each of these geodesics. The fixed point on the geodesic $B_{0,\infty}$ is the point $(0, 0, 1)$ of intersection $B_{0,\infty}$ with geodesic $B_{-1,1}$ which runs from endpoint $(-1, 0, 0)$ to endpoint $(1, 0, 0)$. The based vector is a tangent vector to the geodesic $B_{-1,1}$ at the fixed point in the positive direction. The positive orientation of geodesic $B_{0,\infty}$ is defined in the direction from endpoint $z_0 = (0, 0)$ to endpoint $z_1 = \infty$ on the boundary $C^2 \cup \{\infty\}$. This orientation is inherited for all geodesics A_{g_j} by covering transformations ph_j . To uniform our notation we put ph_0 to be h map. Fixed points on A_{g_j} are points of intersection of A_{g_j} with images of geodesic $B_{-1,1}$ under covering transformations ph_j .

Transformations which correspond to ortholines A_{k_j} take the oriented closed geodesic $A_{f'}$ onto oriented closed geodesics A_{g_j} along A_{k_j} in the positive direction of A_{k_j} . Endpoints $-T_j, T_j$ of ortholines A_{k_j} are antipodal to the origin because the A_{k_j} are perpendicular to geodesic $B_{0,\infty}$. We want to order the endpoints such that ortholines have positive directions at T_j . Endpoints $Z_{j0}, Z_{j1}, -T_j$ and T_j of geodesics A_{g_j} and A_{k_j} lie on a circle because the geodesics intersect each other. We choose the point T_j to be an endpoint such that point $X = [Z_{j0}; Z_{j1}] \cap [-T_j; T_j]$ belongs to the interval $[0; T_j]$. By

straightforward calculations this condition is equivalent to the inequality

$$\left| \begin{array}{cc} x_0 & y_0 \\ x_1 - x_0 & y_1 - y_0 \end{array} \right| \left| \begin{array}{cc} s & t \\ x_1 - x_0 & y_1 - y_0 \end{array} \right| > 0.$$

Here $Z_{j0} = (x_0, y_0) = (ph_j)(0)$, $Z_{j1} = (x_1, y_1) = (ph_j)(\infty)$, $T_j = (s, t)$.

- (6) Now we are ready to calculate the position of the endpoint on the geodesic A_f . The distance from the fixed point on $B_{0,\infty}$ to the orthocurve's endpoint on it is equal to the length of transformation t_j which takes oriented geodesic $B_{-1,1}$ to the oriented orthocurve A_{k_j} . Because the ortholine A_{k_j} intersects $B_{0,\infty}$ orthogonally then the distance is simply

$$\text{length}(t_j) = \text{Log } T_j.$$

The real part of this formula $\log |T_j|$ calculates hyperbolic distance between fixed point and the orthocurve's endpoint. The imaginary part equals to the angle between the based vector and tangent vector to the orthocurve at the point $(0, 0, |T_j|)$.

We consider geodesic A_f as a circle with period $\lambda = \text{Relength}(f)$. Then the ortholine's endpoints on A_f will be mapped onto torus $(-\lambda/2; \lambda/2] \times (-\pi i; \pi i]$.

- (7) Calculations of an endpoint s_j of ortholine A_{k_j} on geodesics A_{g_j} will be done in a similar way. Transformation $(ph)_j^{-1}$ takes oriented geodesic A_{g_j} onto $B_{0,\infty}$ and oriented ortholine A_{k_j} onto geodesic which is orthogonal to $B_{0,\infty}$ and have endpoints $(ph)_j^{-1}(T_j)$, $-(ph)_j^{-1}(T_j)$. Then the position is defined by the formulae

$$\text{length}(s_j) = \text{Log } (ph)_j^{-1}(T_j) + \pi i.$$

We add πi because we need an angle between the fixed vector and the orthocurve but not its tangent vector at the endpoint. For geodesics g_j , the period is $l = \text{length}(g)$ and endpoints belong to the torus $(-l/2; l/2] \times [-\pi i; \pi i]$.

- (8) We sort all ortholines by three parameters:

- (a) distance between geodesics,
- (b) position of endpoints on geodesics A_f and A_g .

Then we eliminate duplicates with identical parameters. Geodesics which start at the same point and go in the same direction coincide. We end up with the list of orthocurves up to real length δ with correct multiplicities.

References

- [1] I. Agol, Volume change under drilling, *Geom. Top.*, **6** (2002), 905–916. [Zbl 1031.57014](#) [MR 1943385](#)
- [2] I. Agol, M. Culler and P. Shalen, Dehn surgery, homology and hyperbolic volume, *Algebr. Geom. Topol.*, **6** (2006), 2297–2312. [Zbl 1129.57019](#) [MR 2286027](#)
- [3] I. Agol, P. Storm and W. Thurston, Lower bounds on volumes of hyperbolic Haken 3-manifolds, *J. AMS*, **20** (2007), no. 4, 1053–1077. [Zbl 1155.58016](#) [MR 2328715](#)
- [4] A. Bearden, *The Geometry of Discrete Groups*, Springer, New York, 1983. [Zbl 0528.30001](#) [MR 698777](#)
- [5] R. Benedetti and C. Petronio, *Lectures on Hyperbolic Geometry*, Springer-Verlag, 1992. [Zbl 0768.51018](#) [MR 1219310](#)
- [6] F. Bonahon, *Low-Dimensional Geometry: From Euclidean surfaces to Hyperbolic Knots*, Student Mathematical Library, 49, IAS/PARK City Mathematical Subseries, 2009. [Zbl 1176.57001](#) [MR 2522946](#)
- [7] A. Champanerkar, J. Lewis, M. Lipyanskiy, S. Meltzer and A. W. Reid, Exceptional regions and associated exceptional hyperbolic 3-manifolds, *Experiment. Math.*, **16** (2007), no. 1, 107–118. [Zbl 1146.57027](#) [MR 2312981](#)
- [8] M. Culler, N. Dunfield and J. Weeks, *SnapPy, a computer program for studying the geometry and topology of 3-manifolds*, 2009. Available at: <http://snappy.computop.org>
- [9] D. Gabai, On the geometric and topological rigidity of hyperbolic 3-manifolds, *J. Amer. Math. Soc.* **10** (1997), 37–74. [Zbl 0870.57014](#) [MR 1354958](#)
- [10] D. Gabai, The Smale conjecture for hyperbolic 3-manifolds: $Isom(M^3) \simeq Diff(M^3)$, *J. Differential Geom.* **58** (2001), no. 1, 113–149. [Zbl 1030.57026](#) [MR 1895350](#)
- [11] D. Gabai, R. Meyerhoff and P. Milley, Minimum volume cusped hyperbolic three-manifolds, *J. Amer. Math. Soc.* **22** (2009), no. 4, 1157–1215. [Zbl 1204.57013](#) [MR 2525782](#)
- [12] D. Gabai, R. Meyerhoff and N. Thurston, Homotopy hyperbolic 3-manifolds are hyperbolic, *Ann. of Math. (2)*, **157** (2003), no. 2, 335–431. [Zbl 1052.57019](#) [MR 1973051](#)
- [13] F. Gehring and G. Martin, Precisely invariant collars and the volume of hyperbolic 3-folds, *J. Differential Geom.* **49** (1998), 411–435. [Zbl 0989.57010](#) [MR 1669657](#)

- [14] O. Goodman, C. Hodgson and W. Neumann, *Home Page For Snap*, 1998. Available at: <http://www.ms.unimelb.edu.au/~snap/>
- [15] C. Hodgson and J. Weeks, Symmetries, isometries and length spectra of closed hyperbolic three-manifolds, *Experiment. Math.*, **3** (1994), no. 4, 261–274. [Zbl 0841.57020](#) [MR 1341719](#)
- [16] K. N. Jones and A. W. Reid, Vol3 and other exceptional hyperbolic 3-manifolds, *Proc. Amer. Math. Soc.*, **129** (2001), no. 7, 2175–2185. [Zbl 0963.57007](#) [MR 1825931](#)
- [17] M. Lipyanskiy, *A computer-assisted application of Poincare's fundamental polyhedron theorem*.
- [18] G. D. Mostow, *Strong Rigidity of Locally Symmetric Spaces*, Ann. of Math. Studies, 78, Princeton Univ. Press, Princeton, NJ, 1973. [Zbl 0265.53039](#) [MR 385004](#)
- [19] A. Przeworski, A universal upper bound on density of tube packings in hyperbolic space, *J. Diff. Geom.*, **72** (2006), 113–127. [Zbl 1098.52005](#) [MR 2215457](#)
- [20] W. P. Thurston, *The Geometry and Topology of Three-Manifolds*, Lecture Notes, Princeton University Mathematics Department, 1979.
- [21] Jeffrey R. Weeks, *SnapPea*, 1993. Available at: <http://geometrygames.org/SnapPea/index.html>

Received June 24, 2013; revised July 14, 2015

D. Gabai, Department of Mathematics, Princeton University, Princeton, NJ 08540, USA
E-mail: gabai@math.princeton.edu

M. Trnkova, Department of Algebra and Geometry, Faculty of Science, Palacky University, Olomouc 772 46, Czech Republic
Current address: Department of Mathematics, California Institute of Technology, Pasadena, CA 91125, USA
E-mail: m.d.trnkova@gmail.com